Journal of Aerosol Science 40 (2009) 1010–1018

Contents lists available at ScienceDirect

Journal of Aerosol Science

journal homepage: www.elsevier.com/locate/jaerosci

Aerodynamic focusing of 5–50 nm nanoparticles in air

Kwang-Sung Lee, Songkil Kim, Donggeun Lee *

School of Mechanical Engineering, Pusan National University, San 30, Jangjeon-dong, Geumjeong-gu, Busan 609-735, Republic of Korea

ARTICLE INFO

Article history:
Received 12 March 2009
Received in revised form
13 August 2009
Accepted 17 September 2009

Keywords:
Aerodynamic lens
Converging–diverging orifices
Aerodynamic focusing

ABSTRACT

An aerodynamic lens consisting of several thin plate orifices has been widely used to focus 30–300 nm nanoparticles. However, there is a big challenge in focusing sub-30 nm particles in air mainly due to flow instability in the lens. Here, we propose a new design of the aerodynamic lens consisting of three converging–diverging orifices to resolve the challenge. Through a series of numerical simulation from single- to multi-lens, we determined a specific design for sub-optimal focusing of 5–100 nm aerosol particles while keeping the air flow stable and free of shock formation. The final multi-lens assembly was revealed to be quite successful.

1. Introduction

Aerodynamic focusing has been widely used to produce a tightly collimated nanoparticle beam in a variety of application fields, such as an efficient inlet for aerosol mass spectrometry (Cho & Lee, 2007; Huffman et al., 2005; Kane & Johnston, 2000; Lee, Cho, & Lee, 2008; Lee, Miller, Kittelson, & Zachariah, 2006; Lee, Park, & Zachariah, 2005; Noble & Prather, 2000) and material syntheses of three-dimensional microstructures (Akedo, Ichiki, Kikuchi, & Maeda, 1998), direct-write fabrication (Akhatov, HOey, Swenson, & Schultz, 2008), implantation of large metal ions (Carrol, Hall, Palmer, & Smith, 1998), and ultra-smooth thin films (Haberland et al., 1995). An aerodynamic lens (ADL) consisting of a series of thin-plate (T-P) orifices, first invented by Liu, Ziemann, Kittelson, and McMurry (1995a, 1995b), has been extensively demonstrated to produce a narrower beam of particles in a wider size range with less transport loss than a capillary (Murphy & Sears, 1964) or a sonic/supersonic nozzle (Crujicic, Zhao, Tong, DeRosset, & Helfritch, 2004; Jen, Pan, Li, Chen, & Cui, 2006; Rafreshi et al., 2002; Whalen, 1987).

Despite these great benefits, there is a big challenge in focusing sub-30 nm aerosol particles, mainly due to their small inertia and high diffusivity. In respect to growing significances of the sub-30 nm nuclei-mode aerosols such as their promising physico-chemical properties and adverse health effect (Lee et al., 2006), a need for an efficient ADL enabling to focus such small particles is rapidly growing too. The gas flow in the ADL is generally restricted to be continuum and subsonic for focusing the nanoparticles. Regarding these constraints, Wang, Kruis, and McMury (2005) suggested an inequality indicating a minimum focusable size of particles $d_{p,\min}$ as

$$d_p \geq \frac{8St_0}{Ma^* Kn^* \rho_p}\left(1+\frac{\pi\alpha}{8}\right)\mu\sqrt{\frac{M}{RT_1\gamma}} = d_{p,min} \propto \frac{St_0}{Ma^* Kn^*}\sqrt{M} \tag{1}$$

where the upper limit of Knudsen number Kn^* was assumed to be 0.1 for the continuum regime, the optimal particle Stokes number St_0 ranged from 0.6 to 1.0 for the T-P orifice (Lee et al., 2008; Wang & McMury, 2006), the critical Mach number

* Corresponding author. Tel.: +82 51 510 2365; fax: +82 51 512 5236.
E-mail address: donglee@pusan.ac.kr (D. Lee).

0021-8502/$ - see front matter © 2009 Elsevier Ltd. All rights reserved.
doi:10.1016/j.jaerosci.2009.09.004

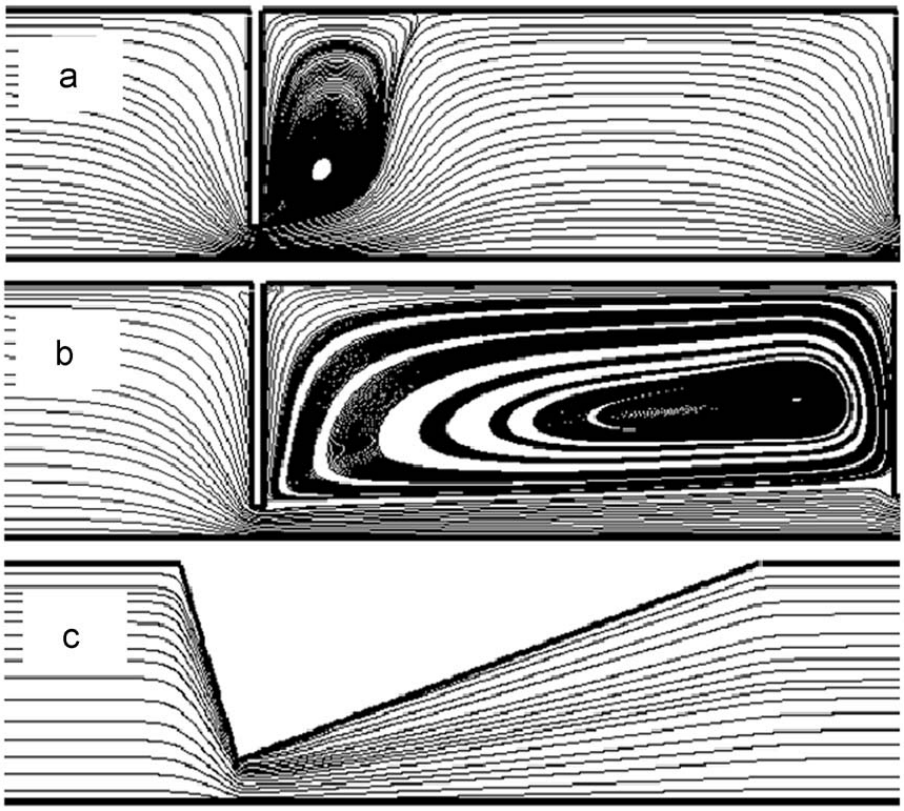

Fig. 1. Comparison of gas streamlines in a thin-plate and a converging–diverging orifice: (a) of He, Re_0=15.5, Ma=0.22, P_{up}=680 Pa, (b) of air, Re_0=116, Ma=0.41, P_{up}=1024 Pa, and (c) of air, Re_0=116, Ma=0.44, P_{up}=880 Pa, α=60°, β=8°. Note that each orifice aperture d_f is 1.24 mm, volume flow rate is 100 sccm and the downstream pressure is 425 Pa.

Ma^* was proportional to the flow discharge coefficient across the T-P orifice C_d ($\leq$0.6; refer to Wang, Kruis, et al. (2005) for the remaining un-described symbols that will not be used in the following).

They attempted to reduce the $d_{p,min}$ by using a lighter carrier gas than air, i.e., reducing the molecular weight of carrier gas M in Eq. (1) and could moderately focus 5–50 nm aerosol particles with a minor change in design with respect to Liu et al. (1995a)'s one. To the best of our knowledge, this is the only available design for aerodynamically focusing sub-30 nm particles. It should be however noted that their promising design works only in He, not in air, mainly due to the constraint of the Mach number (Wang, Kruis, et al., 2005) and the requirement for minimizing flow instability induced by recirculation downstream of the orifice (Wang & McMury, 2006). Since it is impossible to replace the air with He for the environmental aerosols, there still remain a great need for a new design to focus such aerosols *in air.*

Thus returning to Eq. (1), we attempted to decrease the $d_{p,min}$ by increasing the Ma^* and decreasing the St_0. The constraint of the subsonic flow was originally suggested to prevent a shock formation between the orifices which degrades the focusing performance of the T-P orifice. (Wang, Kruis, et al., 2005) Of particular interest is to note that a converging–diverging (C–D) nozzle, well known in aerospace disciplines, has been designed for a shock-free operation even at supersonic flow. In comparison to the T-P orifice, the C–D orifice normally offers superior benefits, e.g., a minimal flow recirculation downstream of the orifice (Wang & McMury, 2006), much lesser pressure drop across the orifice, and the greater discharge coefficient C_d($\sim$1.0) (Whalen, 1987).

These benefits enable the C–D orifice to operate with the minimized flow instability at higher Ma. For this reason, it is in principle expected that the $d_{p,min}$ can be reduced below 10 nm (see Eq. (1)). However, the diverging part of the C–D orifice might increase the length of lens system as well as the residence time of particles, which gives rise to a greater diffusive broadening of particle beam. To circumvent this possibility, the length of C–D orifice should be minimized under the constraints to remain gas flow stable and shock-free. We first show the differences in aspects of flow instability and shock formation when flowing air across the C–D and T-P orifices. We then introduce geometric designing factors of a single C–D orifice and their effects on aerosol focusing. Next we prove this idea with an example that illustrates the use of a new three-stage C–D-type aerodynamic lens to focus 5–50 nm aerosol nanoparticles with a minimal transportation loss.

2. Numerical simulations

A computational fluid dynamics (CFD) software, FLUENT (version 6.2.16), was used to simulate gas flow and particle behavior in the aerodynamic lens. Under typical operation condition of the ADL, inter-particle and particle-to-gas

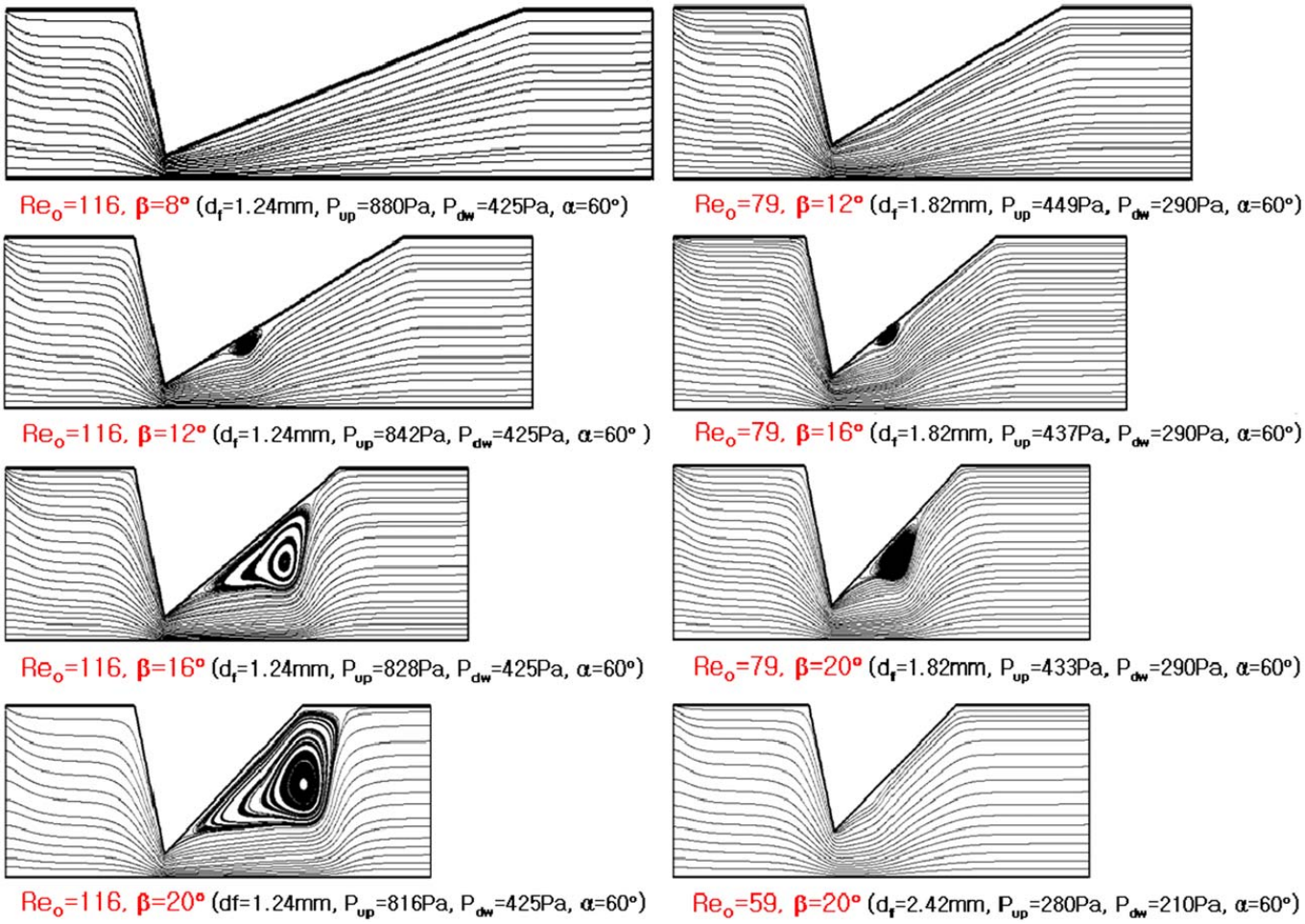

Fig. 2. Development of air-flow recirculation zone in the diverging part of a converging–diverging orifice with different divergent angles of β at various Reynolds numbers and downstream pressures (Q=100 sccm).

interactions have been normally neglected so that the particle-free gas flow field (axisymmetric, steady, compressible, laminar and viscous) can be calculated by solving Navier–Stokes equation and energy equation. Particles with specific sizes are then floated in the flow field to obtain their trajectories and velocities. The CFD calculation was made with the boundary conditions of a constant mass flow rate ($\dot{m} = 2.042 \times 10^{-6}$ kg/s corresponding to 100 sccm air) at the ADL inlet and a constant pressure (10^{-3} Torr) downstream of the ADL outlet, corresponding to typical condition of the ADL assembly in the single particle mass spectrometer (SPMS) (Cho & Lee, 2007; Lee et al., 2005, 2006, 2008). As NaCl nanoparticles has been often used to characterize the SPMS, spherical NaCl nanoparticles with 2 g/cm^3 density are considered in this study. Particle trajectories were obtained with Lagrangian approach including Brownian motion effect (Lee et al., 2008; Wang, Gidwani, Girshick, & McMury, 2005; Wang & McMury, 2006). A user defined function was incorporated with Fluent case files, so as to consider a varying particle slip correction factor C_c at each orifice throat where pressure gradient was largest. A series of grid sensitivity tests were performed as follows. Two uniform grid systems with total number of grids from 50,000 to 100,000 are first tested. In addition, we tested a non-uniform grid system providing denser grids in the vicinity of nozzle, orifice throat and wall. The largest total number of grids tested was more than 300,000. As a result, we confirmed that a stream-wise profile of pressure was varied no larger than 3% as long as total grid numbers is larger than 100,000 in our simulations. It is therefore noted that the non-uniform grid system having 200,000 grids was finally used for the entire simulations in this paper. Other details of the simulation method were described in our previous publication (Lee et al., 2008).

3. Results and discussion

3.1. Issue of gas flow instability

The gas streamlines of He and air across a T-P orifice are compared in Figs. 1a and b at the same volume flow rate (100 sccm for each gas), respectively. In Fig. 1a, the He flow reattaches to the wall shortly after flow separation at the orifice throat and fully develops prior to the next orifice. As such a periodic converging/diverging flow pattern has been

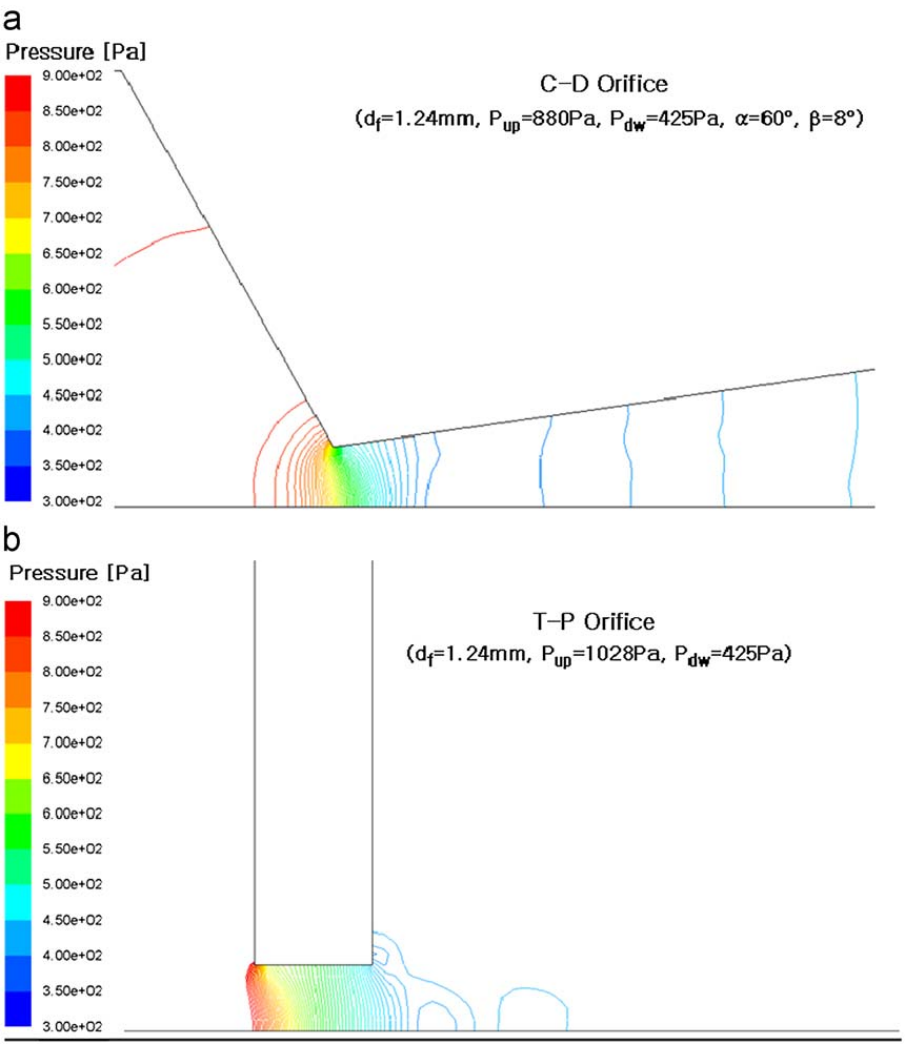

Fig. 3. Pressure contours in air flow across two different orifices with the same aperture of 1.24 mm at Re_0=116 and Q=100 sccm.

acknowledged as a driving force for aerodynamic focusing (Wang, Gidwani, et al., 2005) the He is expected to focus nanoparticles. The air, seven times heavier than the He, however, exhibits a severe flow recirculation downstream of the orifice, which is mainly attributed to seven times greater flow Reynolds number Re ($\propto \dot{m}$). The recirculation zone indeed fills the entire space between the orifices in Fig. 1b, leading to disappearance of the periodic flow pattern and thereby destroying particle focusing (Wang & McMury, 2006). Also Howes, Mackley, and Roberts (1991) reported that if periodic orifice baffles were inserted in a flow tube, stable recirculating vortices forming downstream of each baffle could develop subsequently Kelvin–Helmholtz instability into more complex flow, resulting in an asymmetric flow pattern at a relatively low Reynolds number of order 100.

For this reason, it is required to minimize the recirculation zone, which seems to be impossible unless carrier gas is changed. Interestingly, Fig. 1c shows that a simple replacement of the T-P orifice with the C–D type can resolve this challenge by eliminating the flow recirculation. Flow simulations for four different divergent angles (β=8°, 12°, 16°, 20°) at constant convergent angle of α=60° and an orifice apertures of d_f=1.24 mm reveal in Fig. 2 that the range of $\beta \leq 8°$ is recommended to suppress the flow separation and the resultant vortex formation. When the d_f increases to 1.82 mm, the flow recirculation disappears until $\beta \leq 12°$. The upper limit of β is further increased to 20° at d_f=2.42 mm. From Figs. 1 and 2, it is noted that the higher β does not necessarily shorten the length of the orifice assembly because of longer recirculation zone. On the other hand, as the effect of the convergent angle α on the downstream gas flow was not so significant as that of the β, the α was determined primarily by accounting for particle behavior.

Another requirement in design is to prevent shock formation. Since a normal shock, known as Mach disc (Jen et al., 2006), accompanies a very large pressure gradient, a plot of pressure contour might indicate possible locations of the shock formation. Fig. 3a obviously shows that the air much better accommodates the gradual downstream expansion in contrast to Fig. 3b so that the C–D orifice generates much less pressure gradient. Also, Fig. 3b shows the T-P orifice generates a weak Mach disk causing an abrupt change of air velocity (Lin & Lin, 2007). As such, the shock is unlikely generated in the C-P orifice at least at the present condition. It is noted that the C–D orifice in Fig. 3a corresponds to the first orifice in our multi-lens system where gas speed is maximum as a hardest condition for the design.

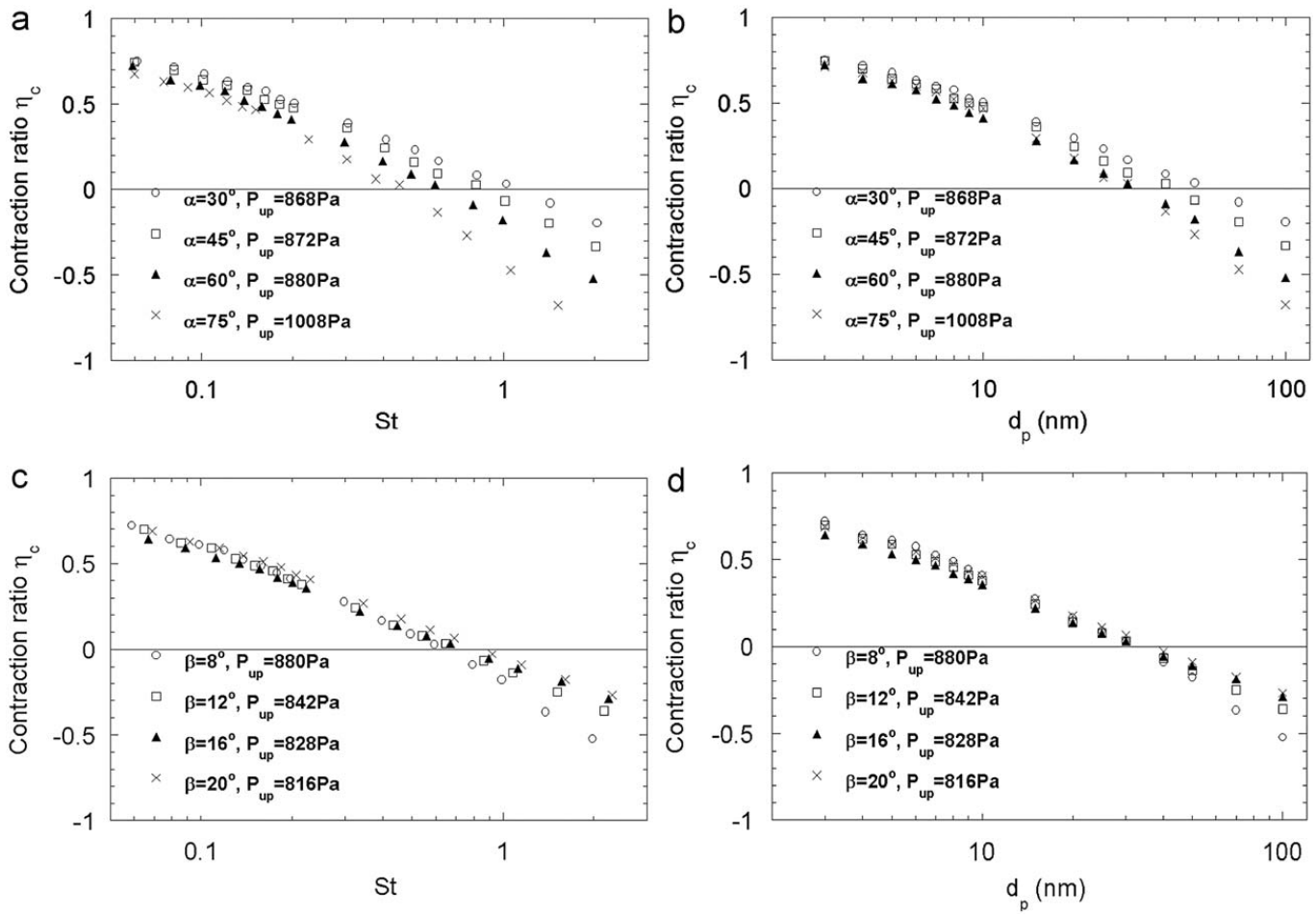

Fig. 4. Effects of geometric angles of the C–D orifice on the contraction ratio: (a) and (b) β=8°, Ma=0.41–0.48, (c) and (d) α=60°, Ma=0.44–0.52. d_f=1.24 mm, Re_0=116, Q=100 sccm and P_{down}=425 Pa.

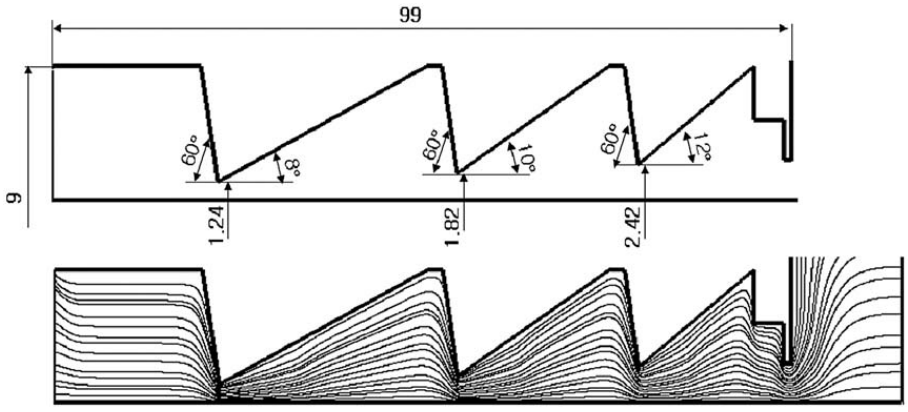

Fig. 5. Schematic of a converging–diverging aerodynamic multi-lens system and gas flow streamlines at Q=100 sccm. The geometric dimensions are in the unit of mm.

3.2. *Effect of orifice configuration on aerosol focusing*

In the aspect of aerosol focusing, the T-P orifice has been evaluated by contraction factor η_c of aerosol beam and transmission efficiency η_t of aerosols across the orifice (Lee et al., 2008; Liu et al., 1995a, 1995b; Wang, Gidwani, et al., 2005; Wang & McMury, 2006). For the T-P orifice, the η_c has been described as a function of *Re*, *Ma* and *St*: $\eta_c=f_1(Re, Ma, St)$ (Wang & McMury, 2006). Despite the lack of the functional form, the St_0 at η_c=0 seemed to be controlled by *Re* and *Ma*. However, as the *Re* and *Ma* are interrelated, one can hardly develop a practical way to reduce the St_0 (Lee et al., 2008; Wang & McMury, 2006). In this regard, we noticed that the C–D orifice has two more independent parameters to control it as $\eta_c=f_2(Re, Ma, St, \alpha, \beta)$ and St_0=g(Re, Ma, α, β).

Table 1
Summary of flow Reynolds and Mach numbers at each orifice throat and nozzle exit in the final multi-lens design.

	1st orifice	2nd orifice	3rd orifice	Nozzle
Re_0	116	79	59.4	52.9
Ma	0.44	0.23	0.15	0.75

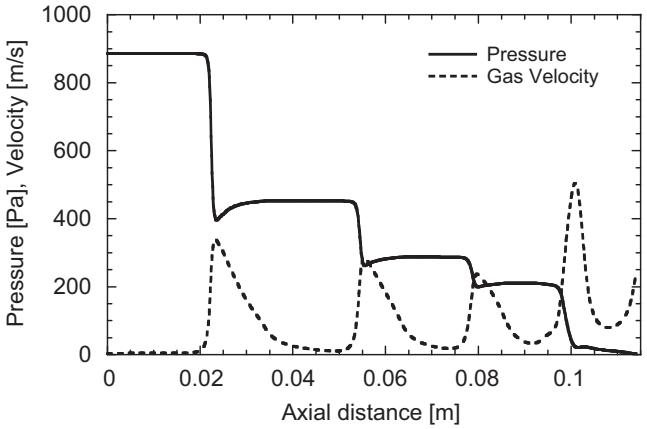

Fig. 6. Profiles of pressure and gas velocity along the lens axis.

Fig. 4a shows the behaviors of the η_c as a function of the particle Stokes number St, for four different angles of α when β=8°. The St_0, the x-intercept at η_c=0, decreases from 1.0 to ~0.4 with increasing the α from 30° to 75°, corresponding to the decrease of the optimal particle size d_{p0} from 50 to 30 nm, respectively, as confirmed in Fig. 4b. The angle of 60° showing the smallest d_{p0} and lower slope than at α=75° is recommended because the less St-dependency of η_c enables the better sub-optimal operation of orifice (Wang, Gidwani, et al., 2005; Wang, Kruis, et al., 2005; Wang & McMury, 2006). At α=30°, the incidence angle of particles approaching to the symmetric axis is too small for best focusing sub-10 nm particles, leading to bouncing them away from the axis to some degree. Once the incidence angle is sufficient (α=60°), further increase of the incidence angle can cause overfocusing of large particles and thereby increasing the slope in Fig. 4a a little more.

On the other hand, the effect of the divergent angle β on the η_c was investigated for four different angles of the β when α=60°, as shown in Figs. 4c and d. Unlike for the α, as the β decreases from 20° to 8°, the St_0 very slightly decreases from 0.85 to 0.6 while the d_{p0} hardly varies from 30 nm. At $\beta \leq 8°$ not allowing the flow recirculation (refer to Fig. 2), the less divergent wall of the C–D orifice greatly reduces outward radial velocities of gas flow which is of particular concern for focusing sub-10 nm particles, leading to the smallest St_0 at β=8°. Whereas, at $\beta \geq 12°$, a pair of recirculating vortices developing along the divergent wall suppress and parallelize the gas streamlines to the symmetric axis so that the radial gas velocity can be reduced more than at β=8°. At the same time, taking a close look at streamlines and particle trajectories, we noticed that near the end of the vortex, the air again undergoes sudden expansion to increase the outward gas velocity, depending on the shape of the vortex. These two trade-off effects are counterbalanced at $\beta \geq 12°$. This is why the values of St_0 or d_{p0} are almost invariant in the range of β. Recalling the requirements for design, i.e., to minimize flow instability ($\beta \leq 8°$) as well as the St_0, we determined the angles of α and β to be 60° and 8°, respectively.

3.3. Design of multi-lens system and an issue of particle diffusion

Though the lower divergent angle was desired in the preceding section, such a lens design obviously increases the length of a multi-lens assembly as well as residence time of aerosols. This inevitably degrades the aerodynamic focusing due to a worsen diffusive broadening that is characterized by a rms value of diffusive displacement of aerosols (Wang & McMury, 2006) as

$$X_{rms} = \sqrt{2Dt} \tag{2}$$

where D is a particle diffusion coefficient expressed by Stokes–Einstein equation and t corresponds to a residence time of aerosols in a multi-lens system. Eq. (2) gives an idea to reduce the undesirable effect of diffusion : reducing X_{rms} by decreasing D and t. The diffusion coefficient D is roughly inversely proportional to a working pressure P through a term of slip correction factor C_c. From a preliminary study, sub-10 nm particles show the greater diffusive motion where the pressure is lower. Hence, it is required to increase the pressure as well as decrease the residence time in the region at the same time. We consider a three-stage C–D type multi-lens system as Wang, Gidwani, et al. (2005) and Liu et al. (1995b) did.

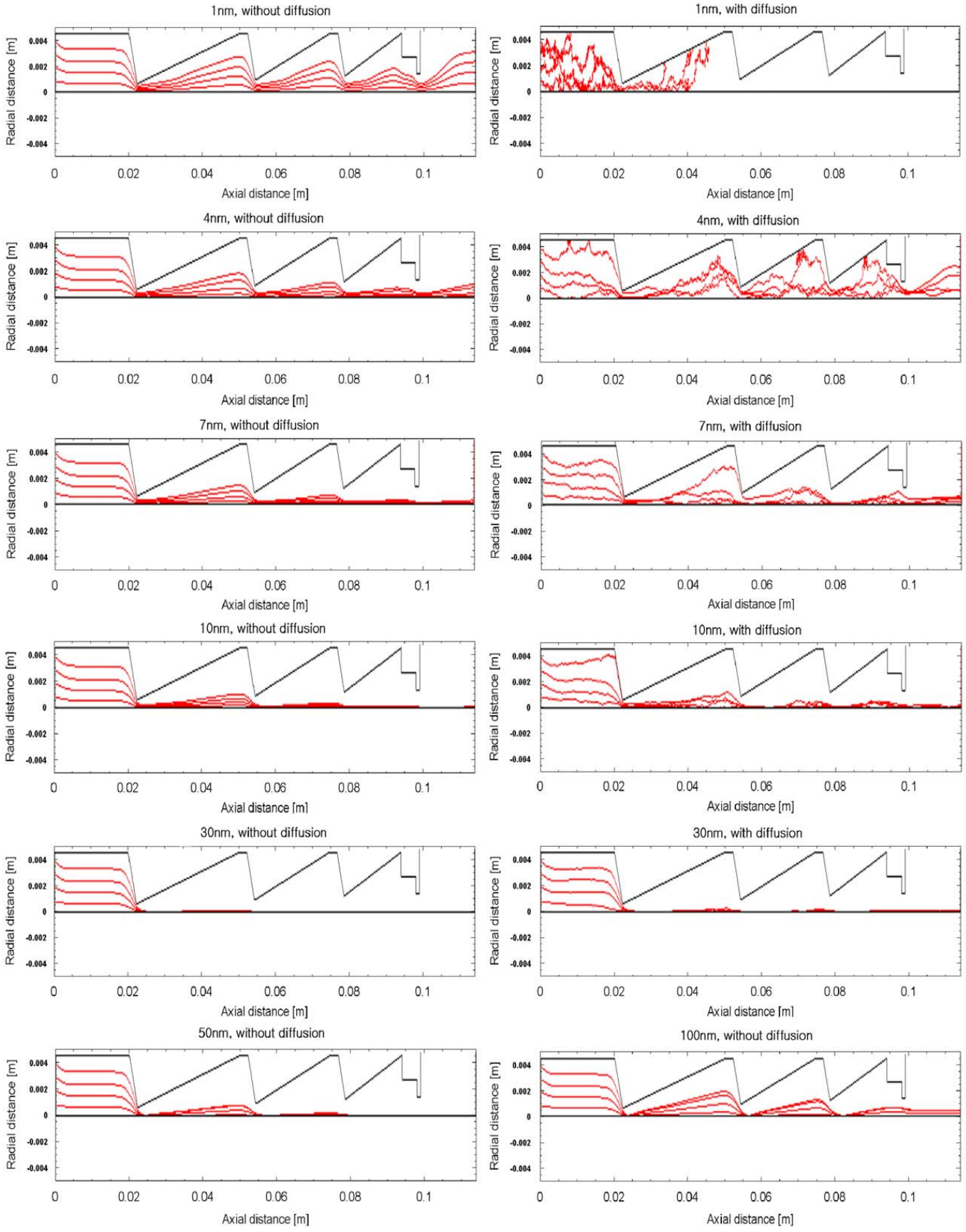

Fig. 7. Size-resolved particle trajectories in the three-stage converging–diverging-type lens assembly with and without diffusion.

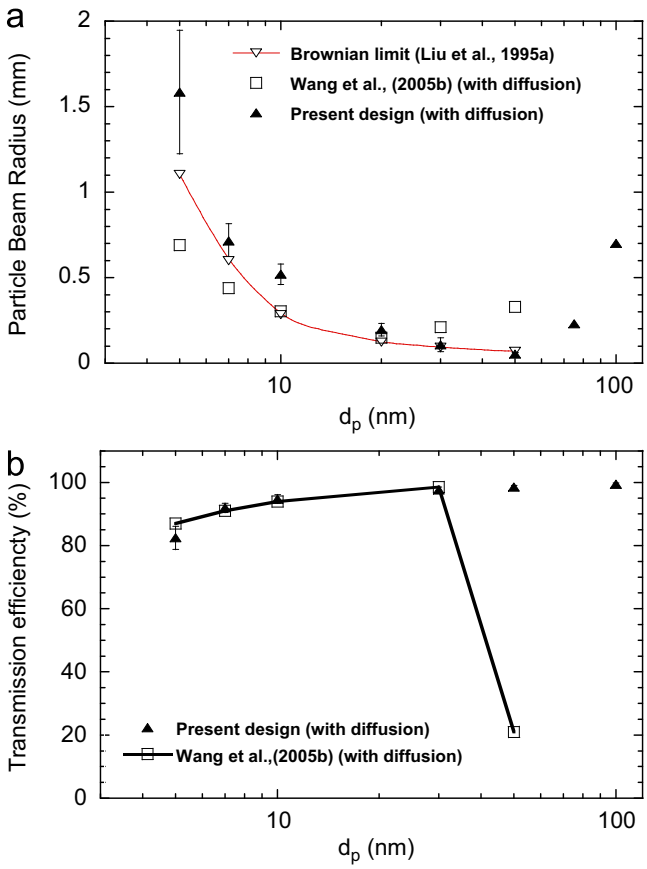

Fig. 8. Performance evaluation of the new aerodynamic lens assembly to focus 5–100 nm particles.

In an effort to reduce the residence time, the angle of β is set to increase gradually from 8° to 12°, from the first to the third C–D orifice, together with minimizing the length of spacers. This particular design, if orifice aperture is set to be constant, redevelops a small recirculating zone downstream of the third orifice. Interestingly, Fig. 2 indicated that the maximum allowable angle of β for the stability issue increases from 8° to 20° with decreasing the Reynolds number. Thus, the aperture of the third orifice is set to 2.42 mm, to lower the *Re* to 59 from 117 at the first orifice (d_f=1.24 mm). Moreover, it should be noted that particles near the symmetric axis are drifted much faster than the off-centered particles, due to a radial variation of the flow velocity. In other words, if sub-10 nm particles are more effectively focused at the first orifice, we may be able to reduce the residence time greatly. Given the relationship of $d_{p0} \propto d_{f0}^3 \, P_{up}{}^2 \, St_0$, the minimal aperture 1.24 mm of the first orifice is matched with this designing effort. The second orifice aperture is set to 1.82 mm, the middle value of the first and third orifices.

The configuration of our novel ADL assembly is described in Fig. 5 (not to scale). Fig. 5 also verifies that the C–D type lens assembly works at a vortex-free condition. According to Wang, Gidwani, et al. (2005), such an ascending-aperture size design operates with large pressure drops. This implies, for a fixed exit pressure of the nozzle, that the upstream pressure of the nozzle, where particles are subject to the greatest diffusion, can be increased as compared to the conventional descending-size design. Overall, the unique design most likely meets the design requirements: (1) minimal flow instability, (2) shock-free operation, (3) minimal particle diffusion. For reference, Table 1 lists flow Reynolds number and Mach number at each orifice throat and nozzle exit and Fig. 6 shows profiles of pressure and gas velocity along the lens axis.

Fig. 7 shows size-resolved particle trajectories in the absence and presence of particle diffusion. Apparently, our C–D type lens system fails to focus particles under 4 nm. However, 7 nm and larger particles are reasonably focused. For the focusable particles, Fig. 4 indicates that the contraction ratio η_c of the first orifice safely lies in the range of $-0.5 \leq \eta_c \leq 0.5$, suggesting that the entire multi-lens system operates sub-optimally for the successful focusing. (Wang, Gidwani, et al., 2005; Wang, Kruis, et al., 2005) Given the particle trajectories in Fig. 7, the final beam width and the transmission efficiency of aerosol particles are calculated as a function of particle size and compared with Wang, Gidwani, et al. (2005)'s data in Fig. 8. For a fair comparison, both of the data are estimated at an equal position, i.e., 5.4 nozzle diameter downstream of the nozzle exit. It is noted that particle trajectories and their resultant beam width are often varied to some extent due to the inherent random nature of diffusion. This trend becomes more prominent for smaller particles. Thus, a data point and its error bar in Fig. 8a denote an average and standard deviation of the beam width from 20 runs of trajectory simulations for each sized particles. Fig. 8 clearly shows that the present design works moderately for focusing 5–100 nm aerosols with an excellent transmission efficient, though sub-10 nm particles are somewhat less focused as compared to Wang et al.'s design working with *He* gas.

4. Conclusion

In this study, we developed a new type of aerodynamic lens system which enables to focus 5–50 nm aerosol nanoparticles in air which has never been achieved before. On the basis of the functional relationship between the minimal focusable particle size $d_{p,min}$ and dimensionless design parameters, we attempted to reduce the $d_{p,min}$ by decreasing optimal Stokes number St_0 and increasing the limit of Mach number. The converging–diverging orifice could greatly reduce flow instability and the possibility of shock formation that has been thought as a big huddle to use the conventional aerodynamic lens in air. The single lens analysis exploring the effect of the lens geometric factors such as convergent and divergent angles was extended to multi-lens together with an extensive effort to minimize particle diffusion effect, resulting in the final design of the lens system. Finally, the new lens system was revealed to work moderately for focusing 5–50 nm particles in air.

Acknowledgement

This work was supported by Core Environmental Technology Development Project for the Next Generation (Project No. 102-071-058).

References

Akedo, J., Ichiki, M., Kikuchi, K., & Maeda, R. (1998). Jet modeling system for realization of three-dimensional micro-structure. *Sensors and Actuators A: Physical*, *69*, 106–112.

Akhatov, I. S., HOey, J. M., Swenson, O. F., & Schultz, D. L. (2008). Aerosol focusing in micro-capillaries: Theory and experiment. *Journal of Aerosol Science*, *39*(8), 691–709.

Carrol, S. J., Hall, S. G., Palmer, R. E., & Smith, R. (1998). Energetic impact of size-selected metal cluster ions on graphite. *Physical Review Letters*, *81*(17), 3715–3718.

Cho, S.-W., & Lee, D. (2007). An ion optics for effective ion detection in single particle mass spectrometry. *Rapid Communications in Mass Spectrometry*, *21*(20), 3286–3294.

Crujicic, M., Zhao, C. L., Tong, C., DeRosset, W. S., & Helfritch, D. (2004). Analysis of the impact velocity of powder particles in the cold-gas dynamic-spray process. *Materials Science and Engineering A*, *368*, 222–230.

Haberland, H., Leber, M., Moseler, M., Qiang, Y., Rattunde, O., Reiners, T., et al. (1995). A new low temperature thin film deposition process: Energetic cluster impact (ECI). *Materials Research Society Symposium Proceedings*, *388*, 207–214.

Howes, T., Mackley, M. R., & Roberts, E. P. L. (1991). The simulation of chaotic mixing and dispersion for periodic flows in baffled channels. *Chemical Engineering Science*, *46*, 1669.

Huffman, J. A., Jayne, J. T., Drewnick, F., Aiken, A. C., Onasch, T., Worsnop, D. R., et al. (2005). Design, modeling, optimization, and experimental tests of a particle beam with probe for the aerodyne aerosol mass spectrometer. *Aerosol Science and Technology*, *39*, 1143–1163.

Jen, T.-C., Pan, L., Li, L., Chen, Q., & Cui, W. (2006). The acceleration of charged nano-particles in gas stream of supersonic de-Laval-type nozzle coupled with static electric field. *Applied Thermal Engineering*, *26*, 613–621.

Kane, D. B., & Johnston, M. V. (2000). Size and composition biases on the detection of individual ultrafine particles by aerosol mass spectrometry. *Environmental Science and Technology*, *34*(23), 4887–4893.

Lee, K.-S., Cho, S.-W., & Lee, D. (2008). Development and experimental evaluation of aerodynamic lens as an aerosol inlet of single mass spectrometry. *Journal of Aerosol Science*, *39*(4), 287–304.

Lee, D., Miller, A., Kittelson, D., & Zachariah, M. R. (2006). Characterization of metal-bearing diesel nanoparticles using single particle mass spectrometry. *Journal of Aerosol Science*, *37*(1), 88–110.

Lee, D., Park, K., & Zachariah, M. R. (2005). Determination of size distribution of polydisperse nanoparticles with single particle mass spectrometry: The role of ion kinetic energy. *Aerosol Science and Technology*, *39*, 162–169.

Lin, S.-L., & Lin, J. (2007). Flow characteristics and micro-scale metallic particle formation in the laser supersonic heating technique. *Optics and Laser Technology*, *39*, 53–60.

Liu, B., Ziemann, P. J., Kittelson, D. B., & McMurry, P. H. (1995). Generation particle beams of controlled dimensions and divergence: I. Theory of particle motion in aerodynamic lenses and nozzle expansions. *Aerosol Science and Technology*, *22*, 293–313.

Liu, B., Ziemann, P. J., Kittelson, D. B., & McMurry, P. H. (1995). Generation particle beams of controlled dimensions and divergence: II. Experimental evaluation of particle motion in aerodynamic lenses and nozzle expansions. *Aerosol Science and Technology*, *22*, 314–324.

Murphy, W. K., & Sears, G. W. (1964). Production of particulate beams. *Journal of Applied Physics*, *35*, 1986–1987.

Noble, C. A., & Prather, K. A. (2000). Real-time single particle mass spectrometry: A historical review of a quarter century of chemical analysis of aerosols. *Mass Spectrometry Review*, *19*, 248–274.

Rafreshi, H. V., Benedek, G., Piseri, P., Vinati, S., Barborini, E., & Milani, P. (2002). A simple nozzle configuration for the production of low divergence supersonic cluster beam by aerodynamic focusing. *Aerosol Science and Technology*, *36*, 593–606.

Wang, X., Gidwani, A., Girshick, S. L., & McMury, P. H. (2005). Aerodynamic focusing of nanoparticles: II Numerical simulation of particle motion through aerodynamic lenses. *Aerosol Science and Technology*, *39*, 624–636.

Wang, X., Kruis, F. E., & McMury, P. H. (2005). Aerodynamic focusing of nanoparticles: I. Guidelines for designing aerodynamic lenses for nanoparticles. *Aerosol Science and Technology*, *39*, 611–623.

Wang, X., & McMury, P. H. (2006). A design tool for aerodynamic lens systems. *Aerosol Science and Technology*, *40*, 320–334.

Whalen, M. V. (1987). Low Reynolds number nozzle flow study. *NASA Technical Memorandum*, 100130.